

Synthesis and Characterization of Phenanthrocarbazole-Diketopyrrolopyrrole Copolymer for High-Performance Field-Effect Transistors

Huajie Chen, Yunlong Guo, Xiangnan Sun, Dong Gao, Yunqi Liu, Gui Yu

Beijing National Laboratory for Molecular Sciences, Institute of Chemistry, Chinese Academy of Sciences, Beijing 100190, People's Republic of China

Correspondence to: G. Yu (E-mail: yugui@iccas.ac.cn)

Received 19 December 2012; accepted 22 January 2013; published online 14 February 2013

DOI: 10.1002/pola.26602

ABSTRACT: In this study, we successfully designed and synthesized a novel phenanthro[1,10,9,8-*c,d,e,f,g*]carbazole (PCZ)-based copolymer poly[*N*-(2-octyldodecyl)-4,8-phenanthro[1,10,9,8-*c,d,e,f,g*]carbazole-*alt*-2,5-dihexadecyl-3,6-di(thiophen-2-yl)pyrrolo[3,4-*c*]pyrrole-1,4(2*H*,5*H*)-dione] (PPDPP) with an extended π -conjugation along the vertical orientation of polymer main chain. This polymer exhibited excellent solubility in common solvent and high thermal stability, owning good properties for solution-processed field-effect transistors (FETs). Besides, absorption spectra demonstrated that annealing PPDPP thin films led to obviously red-shifted maxima, indicating the formations of aggregation or orderly π - π stacking in their solid-state films. X-ray diffraction measurements indicated

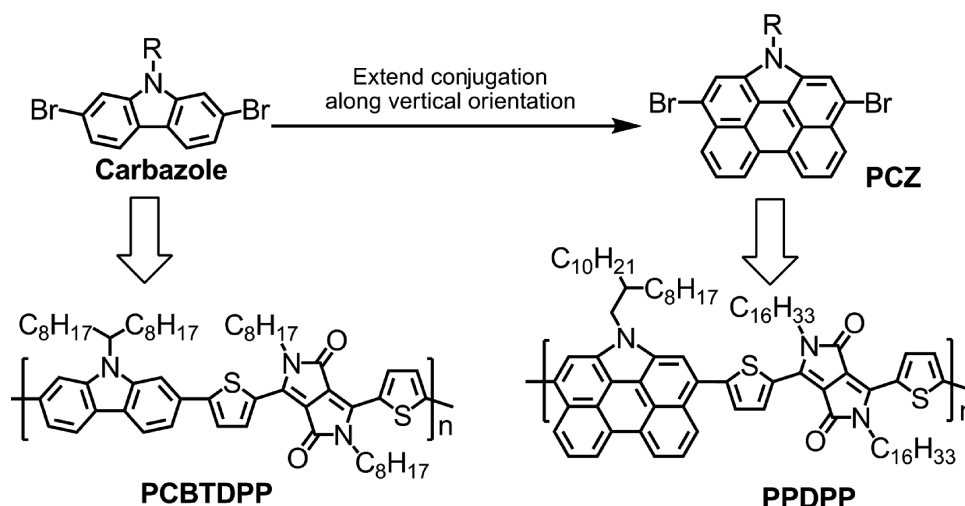
the crystallinity of PPDPP thin films was enhanced after high temperature annealing, which was favorable for charge transport. The solution-processed PPDPP-based FET devices were fabricated with a bottom-gate/bottom-contact geometry. A high hole mobility of up to 0.30 cm²/Vs and a current on/off ratio above 10⁵ had been demonstrated. These results indicated that the copolymers constructed by this kind of ladder-type cores could be promising organic semiconductors for high-performance FET applications. © 2013 Wiley Periodicals, Inc. *J. Polym. Sci., Part A: Polym. Chem.* **2013**, *51*, 2208–2215

KEYWORDS: diketopyrrolopyrrole; field-effect transistors; high performance; ladder-type; phenanthro[1,10,9,8-*c,d,e,f,g*]carbazole

INTRODUCTION Polymer field-effect transistors (FETs) have attracted significant attention because of their potential applications for achieving flexible and low-cost photoelectronic devices through large-scale solution deposition techniques.^{1–4} Recently, Apart from the optimizations of device engineering, the development of novel polymer semiconductors still play a key role to obtain high charge mobility for FETs.^{1–4} An important design principle for developing high-performance polymers is to achieve strong π - π stacking structures, which determine the charge-transporting characteristic in their solid-state films. Usually, to ensure strong intermolecular interactions between the neighboring polymer main chains, the incorporation of π -extended fused-rings should be one of the most effective design strategies.^{5–12} Consequently, an increasing number of ladder-type fused-rings with forced coplanarity structures have been reported to develop some excellent copolymers for the applications in high-performance FETs.^{13–20} However, the realization of this kind of chemical structures generally suffers from synthetic challenges, and thus requires complex molecular design. Furthermore, most ladder-type cores are designed and synthesized according to a conventional approach, namely,

extending π -conjugated structures along the parallel orientation of polymer main chains.^{13–20} For example, Hsu and his coworkers had successfully developed a series of ladder-type dithienosilolo-carbazole (DTSC), dithienopyrrolo-carbazole (DTPC), and dithienocyclopenta-carbazole (DTCC) units, in which two adjacent thiophene units were covalently fused to the central 2,7-carbazole cores along the parallel orientation. The polymers (PDTCCBT, PDTSCBT, and PDTPCBT), constructed from these ladder-type units, exhibited a good charge transporting characteristic, with the hole mobility range from 6.1×10^{-4} to 0.11 cm²/V s.¹⁸ Despite a large number of reports on the copolymers constructed by some ladder-type cores,^{13–20} there are very few studies on the ladder-type cores extending π -conjugation along the vertical orientation of polymer main chains. Therefore, strategies to further develop novel ladder-type π -conjugation cores and their polymers, and thoroughly study structure-performance relationships are well worth exploring for researchers.

Herein, we designed and synthesized a novel ladder-type phenanthro[1,10,9,8-*c,d,e,f,g*]carbazole (PCZ) building-block by extending π -conjugation along the vertical orientation of 2,7-



SCHEME 1 Chemical structures of carbazole, **PCZ**, **PCBTDP**, and **PPDP**.

carbazole core (see Scheme 1). The electron-rich **PCZ** derivative unit was copolymerized with an electron-deficient diketopyrrolopyrrole (**DPP**) unit by Suzuki Coupling to afford an alternating donor–acceptor (D–A) copolymer, poly[*N*-(2-octyldodecyl)-4,8-phenanthro[1,10,9,8-*c,d,e,f,g*]carbazole-*alt*-2,5-dihexadecyl-3,6-di(thiophen-2-yl)pyrrolo[3,4-*c*]pyrrole-1,4(2*H*,5*H*)-dione] (**PPDPP**) (see Scheme 2). Herein, the **DPP** building-block was used as an electron acceptor; because its backbone’s coplanarity would be favorable for strengthening intermolecular π - π stackings.^{21,22} Compared with carbazole core, **PCZ**-based polymers would have much larger π -conjugation structure and stronger electron-donating ability, but weaker solubility. To solve low solubility issue and enhance self-organization, long branched 2-octyldodecyl side chains and hexadecyl side chains are substituted on the nitrogen atoms of **PCZ** and **DPP** units, respectively. Previous works had demonstrated a D–A low bandgap polymer (**PCBTDP**, see Scheme 1), containing carbazole and **DPP** units, exhibited hole mobility of 0.02 cm²/Vs.²³ Herein, the highly π -extended polymer, **PPDPP** with large π -conjugated **DPP** and ladder-type **PCZ** units, exhibited higher hole mobility of up to 0.30 cm²/Vs, along with a current on/off ratio above 10⁵. The enhanced mobility demonstrated that the extension of π -conjugation along the vertical orientation should be a versatile approach to develop novel ladder-type fused heteroarenes.

EXPERIMENTAL

General Measurement and Characterization

Nuclear magnetic resonance (NMR) spectra were conducted on a Bruker ARX-400 spectrometer. Elemental analyses were recorded on a Carlo Erba model 1160 elemental analyzer. MALDI-TOF mass spectrometric measurements were performed on Bruker Biflex III MALDI-TOF. Electron-impact mass spectra (EIMS) were performed on a Bruker BIFLEX III mass spectrometer. Gel permeation chromatography (GPC) was conducted on a waters 515–2410 at 30 °C, using THF as eluent and polystyrenes as reference standard. UV-vis-NIR absorption spectra were measured on a Hitachi U-3010 spec-

trophotometer. Cyclic voltammetry (CV) measurements were recorded on an electrochemistry workstation (CHI660A, Chenhua Shanghai) to determine electrochemical redox potentials. The working electrode was a Platinum stick, coated with a layer of polymer thin film. Platinum wire was used as the counter electrode. Ag/AgCl (Ag in a 0.01 mol/L KCl) electrode was used as the reference electrode. An anhydrous solution 0.1 M tetrabutylammonium hexylfluorophosphate (Bu₄NPF₆) in acetonitrile was used as the electrolyte. Thermal gravity analyses (TGA) were carried out on a TA Instrument Q600 analyzer with a heating and cooling rate of 10 °C/min under an inert atmosphere. Differential scanning calorimetry analyses (DSC) were recorded on a METTLER TOLEDO Instrument DSC822 calorimeter with a heating/cooling rate of 10 °C/min under an inert atmosphere. Atomic force microscopy (AFM) measurements were carried out on a Digital Instruments Nanoscope V instrument, and operated in a tapping mode. X-ray diffraction (XRD) measurements were carried out in a reflection mode, using a D/MAX-TTR III Rigaku X-ray diffraction system.

Fabrication and Measurement of FET Devices

To investigate the charge transporting properties of **PPDPP** thin-film, bottom-gate/bottom-contact (BGBC) FET devices were fabricated using n⁺-Si/SiO₂ substrates (300 nm). The gold (Au) source-drain electrodes were prepared by a photolithography technique to control the channel length (*L*) and channel width (*W* = 1400 μm). Here, different channel lengths of FET devices (*L* = 5 and 50 μm) were investigated to optimize device performance. First, the SiO₂ substrates were washed with ultrasonication in acetone, a cleaning agent, deionized water, and *iso*-propanol, respectively. The cleaned substrates were then dried at 80 °C under vacuum. To form a layer of octadecyltrichlorosilane (OTS) monolayer, OTS-modification was performed on the SiO₂ gate dielectrics in a vacuum. After that, a layer of **PPDPP** thin film (40 nm) was deposited on the OTS-modified SiO₂ substrates by spin-coating a **PPDPP** solution in *o*-dichlorobenzene (10 mg/mL) with a speed of 2000 rpm for 60 s. For annealing FETs, the

samples were placed on a hotplate for 5 min in air directly. The FETs characteristics of the devices were also determined in air by using a Keithley 4200 SCS semiconductor parameter analyzer. The mobility of the devices was calculated in the saturation regime. The equation is listed as follows:

$$I_{DS} = (W/2L)C_i\mu(V_{GS} - V_{th})^2$$

where W/L is the channel width/length, C_i is the insulator capacitance per unit area, and V_{GS} and V_{th} are the gate voltage and threshold voltage, respectively.

Materials

All starting materials were purchased from Aldrich, Alfa, and used directly without further purification. Tetrahydrofuran (THF) and toluene were dried from benzophenone ketyl and sodium. 3,6-Bis-(5-bromo-thiophen-2-yl)-2,5-dihexadecylpyrrolo[3,4-*c*]pyrrole-1,4(2*H*,5*H*)dione (**M2**) was synthesized according to the reported literature.⁵

Nitroperylene (1)

At 60 °C, to a solution of perylene (30.0 g, 119 mmol) in 1 L of 1,4-dioxane was added a mixture of 24 mL of water and 15.0 mL of nitric acid ($d = 1.5$).²⁴ The resulting solution was stirred at 60 °C for 40 min, and then poured into 1.5 L of water. The resulting mixture was filtered and washed with 200 mL of water and 200 mL of ethanol. The red solid was further purified by column chromatography on silica gel (petroleum ether/CH₂Cl₂ = 2:1) to afford a red solid (10.6 g, 30%).

¹H NMR (400 MHz, DMSO): δ (ppm) 8.52 (dd, 2 H), 8.01–7.93 (m, 4 H), 7.81 (d, 1 H), 7.76 (dd, 2 H), 7.66 (t, 1 H), 7.56 (t, 1 H). ¹³C NMR (DMSO, 100 MHz): δ (ppm) 146.0, 134.3, 133.8, 131.3, 130.2, 129.0, 128.9, 128.8, 128.0, 127.8, 127.6, 127.2, 126.8, 125.6, 124.8, 122.8, 122.7, 122.2. EIMS ((*M/z* (%))): 297 [*M*⁺]. Anal. Calcd. for C₂₀H₁₁NO₂: C, 80.80; H, 3.73; N, 4.71; found: C, 80.58; H, 3.68; N, 4.74.

6*H*-phenanthro[1,10,9,8-*c,d,e,f,g*]carbazole (2)

A mixture of 5.0 g (16.8 mmol) of 1-nitroperylene (**1**) and 30 mL of triethyl phosphite was stirred at 160 °C under nitrogen for 5 h.²⁴ After cooling down to room temperature, the reactant was precipitated by addition of 200 mL of petroleum ether, and then filtered to afford the yellow solid. The crude product was further purified by column chromatography on silica gel using CH₂Cl₂ as an eluent to afford a light yellow solid (3.7 g, 83%).

¹H NMR (400 MHz, DMSO): δ (ppm) 12.19 (s, 1 H), 8.76 (d, 2 H), 8.19 (d, 2 H), 7.98 (dd, 4 H), 7.82 (t, 2 H). ¹³C NMR (DMSO, 100 MHz): δ (ppm) 130.6, 129.7, 128.3, 125.0, 124.5, 124.2, 123.5, 120.8, 116.9, 115.5. EIMS ((*M/z* (%))): 265 [*M*⁺]. Anal. Calcd. for C₂₀H₁₁N: C, 90.54; H, 4.18; N, 5.28; found: C, 90.23; H, 4.15; N, 5.21.

N-(2-octyldodecyl)-4,8-dibromo-phenanthro[1,10,9,8-*c,d,e,f,g*]carbazole (4)

A mixture of compound **2** (5.3 g, 20 mmol), NaH (0.72 g, 30 mmol), 1-iodo-2-octyldodecane (12.5 g, 30.6 mmol) in

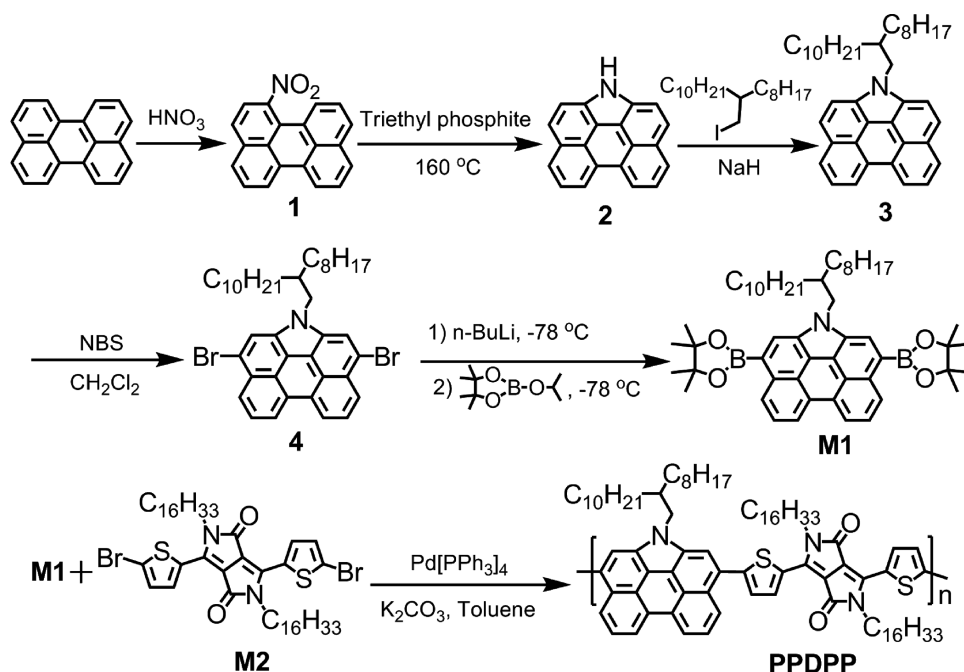
50 mL of dry THF was stirred at 65 °C for 12 h under nitrogen. After cooling to room temperature, the mixture was added 5 mL of water and stirred for 10 min at 0 °C. The resulting mixture was then extracted with diethyl ether. The crude product was purified by chromatography using petroleum ether as an eluent to afford 14 g of yellow oil (**3**) containing some 1-iodo-2-octyldodecane. MALDI–TOF: found 545.8. The proportion of compound **3** was about 78% in this yellow oil, which was determined by ¹H NMR spectra. So the crude product **3** was used directly without further purification. To the solution of compound **3** (14 g, 20 mmol) in 300 mL of CH₂Cl₂ was added NBS (7.48 g, 42 mmol) in four portions. And then the mixture was stirred at room temperature for 3 h. The resulting mixture was then extracted with diethyl ether. The crude product was purified by column chromatography on silica gel (petroleum ether) to yield the yellow solid. The yellow solid was added 100 mL of methanol and sonicated for 10 min, and then filtered to afford the pure product as a light yellow solid (13.4 g, 95%).

¹H NMR (CDCl₃, 400 MHz): δ (ppm) 8.18–8.20 (d, 2 H), 8.04–8.06 (d, 2 H), 7.62–7.65 (t, 2 H), 7.50 (s, 2 H), 3.76–3.78 (d, 2 H), 1.85 (m, 1 H), 1.16–1.26 (m, 32 H), 0.83–0.90 (m, 6 H). ¹³C NMR (CDCl₃, 100 MHz): δ (ppm) 130.83, 129.01, 127.08, 124.93, 124.48, 123.01, 121.16, 117.57, 116.36, 115.19, 49.57, 39.51, 31.93, 31.87, 31.57, 29.85, 29.62, 29.56, 29.51, 29.34, 29.28, 26.34, 22.72, 22.66, 14.18, 14.14. MALDI–TOF: found, 703. Anal. Calcd. for C₄₀H₄₉Br₂N: C, 68.28; H, 7.02; N, 1.99; found: C, 68.39; H, 7.11; N, 1.96.

N-(2-octyldodecyl)-4,8-bis(4,4,5,5-tetramethyl-1,3,2-dioxaborolan-2-yl)phenanthro[1,10,9,8-*c,d,e,f,g*]carbazole (M1)

At –78 °C, to a solution of compound **4** (3.5 g, 5 mmol) in 100-mL dry THF was added dropwise 5.2 mL of 2.5 M solution of *n*-butyllithium (*n*-BuLi) in *n*-hexane. The mixture was stirred at –78 °C for 30 min, then warmed to 0 °C for 1 h, and then cooled down to –78 °C again, 2-isopropoxy-4,4,5,5-tetramethyl-1,3,2-dioxaborolane (2.8 g, 15 mmol) was added rapidly into the solution. The resultant mixture was allowed to stir at room temperature overnight, then quenched with 10 mL of water and extracted with dichloromethane. The organic extracts were washed with brine and dried over magnesium sulfate and concentrated in vacuum. The crude product was purified by chromatography using petroleum ether/dichloromethane (3:1) as an eluent to give a yellow solid. Yield: 1.28 g, 32%.

¹H NMR (CDCl₃, 400 MHz): δ (ppm) 8.97–8.99 (d, 2 H), 8.68–8.70 (d, 2 H), 8.45 (s, 2 H), 7.86 (t, 2 H), 4.64–4.65 (d, 2 H), 2.35 (m, 1 H), 1.49 (s, 24 H), 1.36–1.40 (m, 6 H), 1.19–1.27 (m, 26 H), 0.81–0.87 (m, 6 H). ¹³C NMR (CDCl₃, 100 MHz): δ (ppm) 132.97, 132.41, 130.74, 126.76, 124.99, 124.40, 122.91, 120.66, 119.90, 83.76, 49.91, 39.89, 32.08, 32.05, 31.79, 30.08, 29.80, 29.71, 29.50, 29.45, 26.54, 25.24, 22.84, 22.82, 14.29. MALDI–TOF: found, 797.7. Anal. Calcd. for C₅₂H₇₃B₂NO₄: C, 78.29; H, 9.22; N, 1.76; found: C, 78.01; H, 9.23; N, 1.79.



SCHEME 2 Synthetic routes of the novel ladder-type polymer **PPDPP**.

Poly[*N*-(2-octyldodecyl)-4,8-phenanthro[1,10,9,8-*c,d,e,f,g*]-carbazole-*alt*-2,5-dihexadecyl-3,6-di(thiophen-2-yl)pyrrolo[3,4-*c*]pyrrole-1,4(2*H*,5*H*)-dione] (PPDPP)

Monomer **M1** (0.16 g, 0.2 mmol), monomer **M2** (0.18 g, 0.2 mmol), 2 M aqueous K_2CO_3 solution (5 mL), toluene (10 mL), and three drops of *N*-methyl-*N*, *N*-dioctyloctan-1-ammonium chloride (Aliquat 336) were added into a 50-mL flask. The mixture was charged with nitrogen through a freeze-pump-thaw cycle for three times, and then tetrakis(triphenylphosphine)palladium (20 mg) was added. The mixture was stirred for 48 h at 110 °C under nitrogen atmosphere. Then phenylboronic acid (0.3 g, 2.5 mmol) was added and stirred at reflux for 3 h. Next, bromobenzene (5 mL) was then added under nitrogen, and then the mixture was stirred for another 3 h. After the reactant was cooled down to room temperature, the polymer was precipitated by addition of 200 mL of methanol and 10 mL of hydrochloric acid. The precipitate was filtered and washed by methanol. Finally, the polymer was subjected to Soxhlet extraction with methanol for 12 h, acetone for 12 h, hexane for 12 h, and finally chloroform for 12 h. The evaporation of chloroform fractions afforded a dark solid. Yield: 175 mg, 68%.

1H NMR ($CDCl_3$, 400 MHz): δ (ppm) 8.94–9.35 (br, 2 H), 8.40–8.68 (br, 4 H), 7.51–7.86 (br, 6 H), 3.99–4.55 (br, 6 H), 2.41 (br, 1 H), 1.97–2.03 (br, 4 H), 1.25–1.58 (br, 84 H), 0.86 (br, 12 H). GPC: $M_w = 16.6$ KDa, $M_n = 10.2$ KDa, $M_w/M_n = 1.63$. Anal. Calcd. for $(C_{86}H_{121}N_3O_2S_2)_n$: C, 79.88; H, 9.43; N, 3.25; found: C, 79.42; H, 9.20; N, 3.30.

RESULTS AND DISCUSSION

Synthesis and Characterization

The synthetic routes of monomers and copolymer are presented in Scheme 2. Compounds **1** and **2** were readily

synthesized following a reported procedure,²⁴ which was then converted to compound **3** via alkylation. Then compound **3** was directly brominated to obtain an intermediate **4**. The structure of compound **4** was carefully confirmed by NMR spectra, MALDI-TOF, and elemental analysis. Here, a long branched alkyl-chain substituted on the nitrogen atom of the **PCZ** core was rationally designed for better solubility and self-assembly purpose. Then, compound **4** was converted to monomer **M1** by the present of *n*-BuLi and 2-isopropoxy-4,4,5,5-tetramethyl-1,3,2-dioxaborolane. Another important monomer **M2** was prepared according to a reported literature.⁵ Palladium-catalyzed Suzuki-coupling reaction of **M1** and **M2** was carried out to obtain the target polymer **PPDPP** in 68% yield. After removing the residual catalytic metal and low-molecular-weight oligomers of the resultant polymer by Soxhlet extraction with methanol (12 h), acetone (12 h), and hexane (12 h), the residue was extracted with chloroform to afford copolymer **PPDPP** with weight-average molecular weights (M_w) of 16.6 KDa and polydispersity indexes (PDI) of 1.63. Because of the introduction of long 2-octyldodecanyl and hexadecyl side-chains into polymer backbone, **PPDPP** exhibited excellent solubility (>30 mg/mL, at 25 °C) in common organic solvents, including THF, chloroform, toluene, and chlorobenzene. Moreover, **PPDPP** showed good film-forming ability and could obtain high-quality thin films by simple spin-coating techniques.

Thermal Analysis

To determine the thermal properties of **PPDPP**, TGA, and DSC had been performed under nitrogen. As shown in Figure 1, **PPDPP** exhibits excellent thermal stability with the decomposition temperature (5% weight loss) above 400 °C. This result shows that **PPDPP** matches well with the fabricating needs of organic optoelectronic devices. Besides, DSC

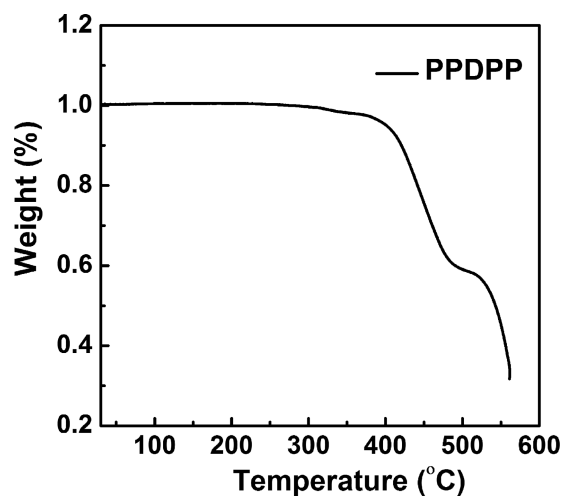


FIGURE 1 TGA curve of PPDPP with a heating rate of 10 °C/min under an inert atmosphere.

measurement of PPDPP reveals no clear liquid-crystalline phase transition from 25 to 300 °C (Fig. 2), however, has a melting transition at 188 °C, which is attributable to the melting of polymer backbone.

Optical Properties

The UV-vis-IR absorption spectra of the dilute PPDPP solution in chloroform and the spin-coated thin film on the quartz glass substrate are presented in Figure 3, and the corresponding data are summarized in Table 1. In the case of chloroform solution, PPDPP displayed a broad absorption band extended from 500 to 850 nm due to the strong intramolecular charge transfer arising from the strong D-A interactions. Compared with the absorption maximum (653 nm) in solution, the absorption peak in the solid-state film was significantly red-shifted to 702 nm. When the thin films were annealed at 120 and 200 °C, the absorption maximum (λ_{max}) were further red-shifted to 714 and 734 nm, respec-

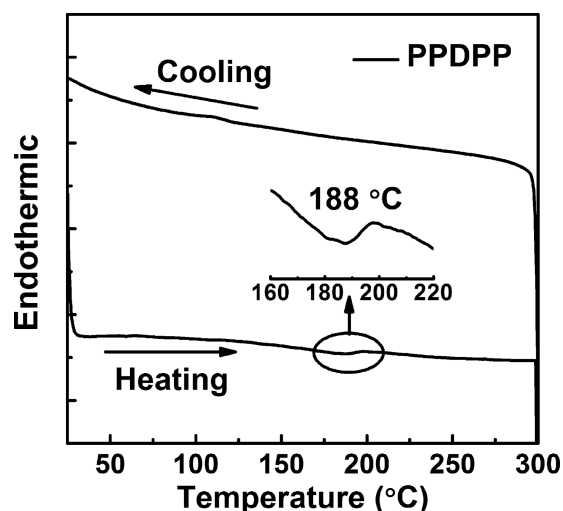


FIGURE 2 DSC curves of PPDPP with a heating rate of 10 °C/min under an inert atmosphere.

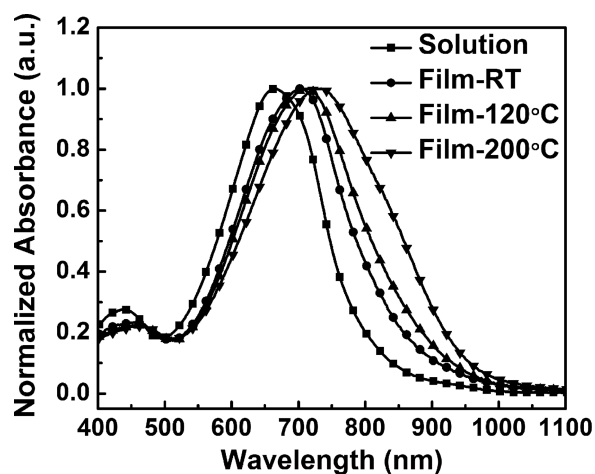


FIGURE 3 The UV-vis-NIR absorption spectra of PPDPP in chloroform solution and thin films annealing at different temperature.

tively. These red-shifted features indicate that the aggregation or orderly π - π stacking occurs in the solid-state film.^{25,26} These results indicate that the annealing treatment would be helpful for enhancing the charge transport in polymer films. Besides, the optical bandgap was estimated to be 1.39 eV, which was calculated from the onset absorption (\sim 890 nm) of polymer thin film without annealing.

Electrochemical Properties

CV measurement revealed that polymer PPDPP exhibited a reversible and strong oxidation process but a weak reduction one, indicating PPDPP might be operated as a *p*-type transporting semiconductor.²⁶ As shown in Figure 4, the onset oxidation potential (E_{ox}) of PPDPP is 0.81 V. The corresponding energy level of the highest occupied molecular orbital (HOMO) is -5.21 eV, which is calculated according to the equation of $E_{\text{HOMO}} = -(E_{\text{ox}}^{\text{onset}} + 4.4)$ eV.²⁷ Combining with the optical bandgap of 1.39 eV, the energy level of lowest unoccupied molecular orbital (LUMO) is determined to be -3.82 eV, calculated according to the equation of $E_{\text{LUMO}} = (E_{\text{HOMO}} + E_{\text{g}}^{\text{optical}})$ eV.²⁷ One can note that this deep-lying HOMO value matches well with the work function of bare gold electrodes (5.13 eV),²⁸ which might facilitate the hole injection from gold electrodes into polymer thin films and thus realize high-performance charge transport.²⁷

Field-Effect Transistor Characteristics

To investigate the carrier transport properties of PPDPP thin film, the FET devices with a conventional BGBC configuration were fabricated. The gold (Au) source-drain electrodes were

TABLE 1 Optical Property and field-Effect Characteristics for PPDPP Thin Film Based on Different Annealing Temperatures

T (°C)	λ_{max} (nm)	M (cm^2/Vs)	$I_{\text{on}}/I_{\text{off}}$	V_{th} (V)
As-spun/25	702	0.035 ± 0.002	$>10^4$	-8 ± 2
120	714	0.063 ± 0.005	$>10^4$	-11 ± 2
200	734	0.13–0.30	10^5 – 10^7	-10 ± 5

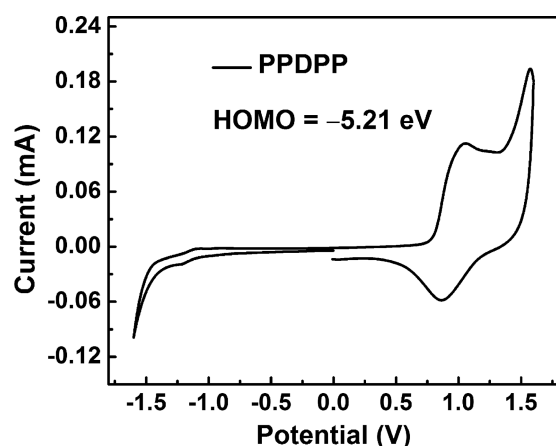


FIGURE 4 Cyclic voltammety of PPDPP film in 0.1 mol/L Bu4NPF6, acetonitrile solution, with a scan rate of 0.1 V/s.

prepared by photolithography method. A layer of PPDPP thin film (40 nm) was then deposited onto OTS-modified Si/SiO₂ (300 nm) substrate by a simple spin-coating technique. Then PPDPP-based FETs were annealed and measured in air directly. Figure 5 shows the typical *p*-type output and transfer curves of PPDPP-based FETs. Data are summarized

in Table 1. The field-effect results showed the FET performance of PPDPP thin film was dependent on annealing temperature, which was consistent with the results of absorption spectra. For the unannealed FET devices with $L = 50 \mu\text{m}$, the average saturation mobilities extracted from transfer curves were equal to $0.035 \text{ cm}^2/\text{Vs}$, with a current on/off ratio of 10^4 . Annealing FET devices at 120 and 200 °C, the average saturation mobilities reached 0.063 and $0.13 \text{ cm}^2/\text{Vs}$, respectively. To further optimize device performance, FET devices with $L = 5 \mu\text{m}$ were investigated under the annealing temperature of 200 °C. The average saturation mobilities extracted from transfer curves reached $0.25 \text{ cm}^2/\text{Vs}$, together with a current on/off ratio above 10^5 and a threshold voltage of -15 V . Some hero transistors exhibited the highest hole mobility of up to $0.30 \text{ cm}^2/\text{Vs}$. Previous work had demonstrated that the molecular weight played a key role in improving charge mobilities, because the thin film crystallinity could be enhanced with growing molecular weight.^{12(b)} Herein, despite relatively low molecular weight for PPDPP ($M_w = 16.6 \text{ KDa}$, PDI = 1.63), the highly π -extended copolymer PPDPP exhibited much higher mobility ($0.30 \text{ cm}^2/\text{Vs}$) compared with PCBTDP ($M_w = 30 \text{ KDa}$, PDI = 2.1, and $\mu = 0.02 \text{ cm}^2/\text{Vs}$), which was higher by one order of magnitude than that of PCBTDP.¹⁵ The results indicated that the

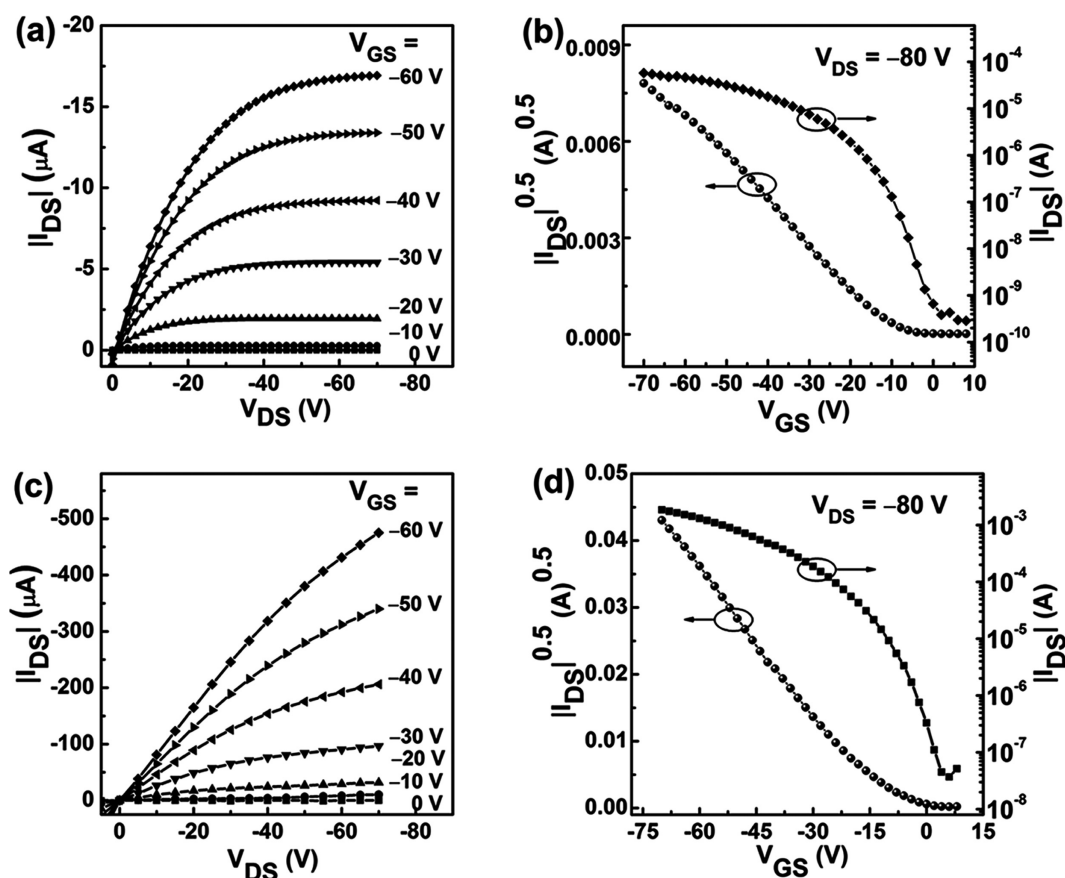


FIGURE 5 Output (a) and transfer (b) curves of PPDPP-based FETs annealing at 200 °C with $W = 1400 \mu\text{m}$ and $L = 50 \mu\text{m}$, exhibiting a hole mobility of $0.13 \text{ cm}^2/\text{Vs}$; Output (c) and transfer (d) curves of PPDPP-based FETs annealing at 200 °C with $W = 1400 \mu\text{m}$ and $L = 5 \mu\text{m}$, exhibiting a hole mobility of $0.30 \text{ cm}^2/\text{Vs}$.

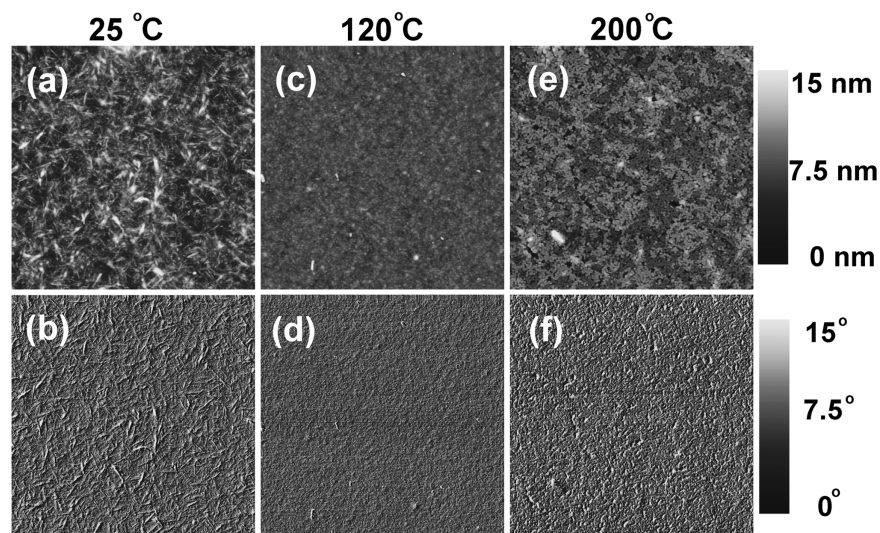


FIGURE 6 AFM topography (top) and phase (bottom) images ($5 \times 5 \mu\text{m}^2$) of **PPDPP** thin films on the OTS-modified SiO_2/Si substrates. (a and b) annealed at 25°C and (c and d) annealed at 120°C , and (e and f) annealed at 200°C .

largely conjugated **PCZ** units and **DPP** units would provide a strong force to facilitate π - π stacking between polymer backbones, therefore successfully enhancing hole transport.

Microstructure of PPDPP Thin Films

To understand the reasons why annealing treatments improved charge-transporting ability, AFM and XRD measurements were used to investigate the change in the microstructure of **PPDPP** thin films upon annealing treatments. AFM images revealed that a uniform and intertwined fiber structure was formed for the as-spun thin films (Fig. 6). This kind of fiber structure is a typical one observed for most conjugated polymer films, like regioregular poly(3-hexylthiophene)²⁹ and **DPP**-based polymers.^{10,30} However, the polycrystalline grains of the annealed thin films were clearly unlike the ones of as-spun films, and were a fine nodule-like structure. This obvious change in film morphology might be caused by polymer backbone's melting. Compared with thin films annealed at 120°C , a larger polycrystalline grains was obtained for the ones annealed at 200°C , which was helpful for charge transport.

Consistent with the annealing-induced changes in their film morphologies, different crystallinity of **PPDPP** was observed by comparing the XRD data of annealed **PPDPP** thin films. Figure 7 shows XRD patterns of **PPDPP** thin films deposited on OTS-modified Si/SiO_2 substrates. For as-spun samples and the ones annealed at 120°C , two diffraction peaks were clearly observed in XRD patterns, suggesting a strong tendency for **PPDPP** thin films to self-assemble into an orderly lamellar structure in solid-state films. Once thin films were thermal annealed at 200°C , thin films displayed clear diffraction peaks up to the third orders, indicating the increases in crystallinity of polymer thin films. Such an increase of crystallinity could be an important reason for the improved charge transporting ability. Besides, a new sharp peak assigned to a-axis ($h00$) direction was observed at $2\theta = 3.36^\circ$ corresponding to a interlayer distance of 26.26 \AA

(100). This interlayer distance (26.26 \AA) is shorter than that of theoretically calculated alkyl side-chain ($\sim 36 \text{ \AA}$).²⁶ Thus, these side-chains should be closely interdigitated with each other between adjacent layers, which is useful for high-performance charge transport.

CONCLUSIONS

In summary, a novel ladder-type copolymer, **PPDPP**, with alkyl substituted **PCZ** unit as an electron donor and **DPP** unit as an electron acceptor, was designed and synthesized by conventional Suzuki-coupling reaction. The long branched alkyl-chains ensured **PPDPP** excellent solubility in most organic solvent, along with good film-forming ability and self-organization ability. UV-vis-IR spectra measurements showed **PPDPP** thin film covered the whole visible light band (from 400 to 900 nm) due to the strong intramolecular charge

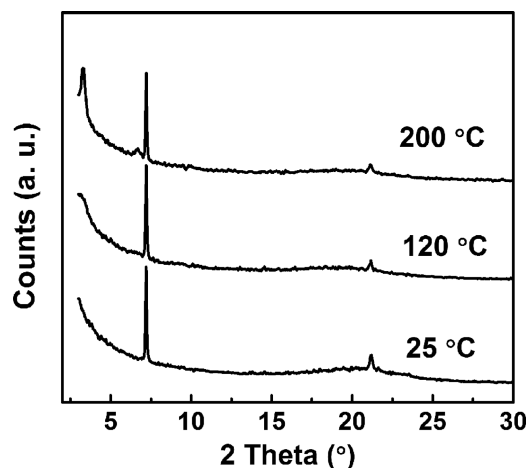


FIGURE 7 X-ray scattering curves of **PPDPP** thin films on the OTS-modified SiO_2/Si substrates under annealing treatments at different temperature.

transfer. Besides, a suitable HOMO energy level of -5.21 eV was favorable for hole injection from source electrode into polymer thin film. The solution-processed FETs based on PPDPP film exhibited good field-effect performance in air. The highest hole mobility reached 0.30 cm^2/Vs with a current on/off ratio above 10^5 , which fully matched with the requirements for fabricating low-cost and flexible display and smart card. This study demonstrated that the extension of π -conjugation along the vertical orientation should be an effective method to develop ladder-type polymer semiconductors for high-performance organic optoelectronic applications.

ACKNOWLEDGMENTS

This work was supported by the National Natural Science Foundation of China (20825208, 61101051, 51233006, and 21021091) and the Major State Basic Research Development Program (2011CB808403 and 2011CB932303).

REFERENCES AND NOTES

- 1 A. Facchetti, *Chem. Mater.* **2011**, *23*, 733–758.
- 2 W. P. Wu, Y. Q. Liu, D. B. Zhu, *Chem. Soc. Rev.* **2010**, *39*, 1489–1502.
- 3 P. M. Beaujuge, J. M. J. Fréchet, *J. Am. Chem. Soc.* **2011**, *133*, 20009–20029.
- 4 Y. G. Wen, Y. Q. Liu, Y. L. Guo, G. Yu, W. P. Hu, *Chem. Rev.* **2011**, *111*, 3358–3406.
- 5 T. L. Nelson, T. M. Young, J. Y. Liu, S. P. Mishra, J. A. Belot, C. L. Balliet, A. E. Javier, T. Kowalewski, R. D. McCullough, *Adv. Mater.* **2010**, *22*, 4617–4621.
- 6 T. Lei, Y. Cao, Y. L. Fan, C. J. Liu, S. C. Yuan, J. Pei, *J. Am. Chem. Soc.* **2011**, *133*, 6099–6101.
- 7 J. G. Mei, D. H. Kim, A. L. Ayzner, M. F. Toney, Z. N. Bao, *J. Am. Chem. Soc.* **2011**, *133*, 20130–20133.
- 8 Y. Zhang, J. Y. Zou, H. L. Yip, K. S. Chen, D. F. Zeigler, Y. Sun, A. K. Y. Jen, *Chem. Mater.* **2011**, *23*, 2289–2291.
- 9 (a) J. Y. Shim, B. H. Lee, S. Song, H. Kim, J. A. Kim, I. Kim, K. Lee, H. Suh, *J. Polym. Sci. Part A: Polym. Chem.* **2013**, *51*, 241–249; (b) J. B. Lee, K. H. Kim, C. S. Hong, D. H. Choi, *J. Polym. Sci. Part A: Polym. Chem.* **2012**, *50*, 2809–2818.
- 10 Y. N. Li, P. Sonar, S. P. Singh, M. S. Soh, M. V. Meurs, J. Tan, *J. Am. Chem. Soc.* **2011**, *133*, 2198–2204.
- 11 I. McCulloch, M. Heeney, C. Bailey, K. Genevicius, I. MacDonald, M. Shkunov, D. Sparrowe, S. Tierney, R. Wagner, W. Zhang, M. L. Chabinyc, R. J. Kline, M. D. McGehee, M. F. Toney, *Nat. Mater.* **2006**, *5*, 328–333.
- 12 (a) H. J. Chen, C. He, G. Yu, Y. Zhao, J. Y. Huang, M. L. Zhu, H. T. Liu, Y. L. Guo, Y. F. Li, Y. Q. Liu, *J. Mater. Chem.* **2012**, *22*, 3696–3698; (b) H. N. Tsao, D. M. Cho, I. Park, M. R. Hansen, A. Mavrinskiy, D. Y. Yoon, R. Graf, W. Pisula, H. W. Spiess, K. Müllen, *J. Am. Chem. Soc.* **2011**, *133*, 2605–2612; (c) X. G. Zhao, Y. G. Wen, L. B. Ren, L. C. Ma, Y. Q. Liu, X. Zhan, W. J. Polym. Sci. Part A: Polym. Chem. **2012**, *50*, 4266–4271.
- 13 X. C. Wang, H. Luo, Y. P. Sun, M. J. Zhang, X. Y. Li, G. Yu, Y. Q. Liu, Y. F. Li, H. Q. Wang, *J. Polym. Sci. Part A: Polym. Chem.* **2012**, *50*, 371–377.
- 14 B. C. Schroeder, Z. G. Huang, R. S. Ashraf, J. Smith, P. D'Angelo, S. E. Watkins, T. D. Anthopoulos, J. R. Durrant, I. McCulloch, *Adv. Funct. Mater.* **2012**, *22*, 1663–1670.
- 15 M. J. Zhang, X. Guo, X. C. Wang, H. Q. Wang, Y. F. Li, *Chem. Mater.* **2011**, *23*, 4264–4270.
- 16 W. M. Zhang, J. Smith, S. E. Watkins, R. Gysel, M. McGehee, A. Salleo, J. Kirkpatrick, S. Ashraf, T. Anthopoulos, M. Heeney, I. McCulloch, *J. Am. Chem. Soc.* **2010**, *132*, 11437–11439.
- 17 I. McCulloch, R. S. Ashraf, L. Biniek, H. Bronstein, C. Combe, J. E. Donaghey, D. I. James, C. B. Nielsen, B. C. Schroeder, W. M. Zhang, *Acc. Chem. Res.* **2012**, *45*, 714–722.
- 18 J. S. Wu, Y. J. Cheng, T. Y. Lin, C. Y. Chang, P. I. Shih, C.-S. Hsu, *Adv. Funct. Mater.* **2012**, *22*, 1711–1722.
- 19 J. S. Wu, Y. J. Cheng, M. Dubosc, C. H. Hsieh, C. Y. Chang, C.-S. Hsu, *Chem. Commun.* **2010**, *46*, 3259–3261.
- 20 Y. J. Cheng, J. S. Wu, P. I. Shih, C. Y. Chang, P. C. Jwo, W. S. Kao, C.-S. Hsu, *Chem. Mater.* **2011**, *23*, 2361–2369.
- 21 O. P. Lee, A. T. Yiu, P. M. Beaujuge, C. H. Woo, T. W. Holcombe, J. E. Millstone, J. D. Douglas, M. S. Chen, J. M. Fréchet, *Adv. Mater.* **2011**, *23*, 5359–5363.
- 22 Y. L. Qiao, Y. L. Guo, C. M. Yu, F. J. Zhang, W. Xu, Y. Q. Liu, D. B. Zhu, *J. Am. Chem. Soc.* **2012**, *134*, 4084–4087.
- 23 Y. P. Zou, D. Gendron, R. Badrou-Aïch, A. Najari, Y. Tao, M. Leclerc, *Macromolecules* **2009**, *42*, 2891–2894.
- 24 W. Jiang, H. L. Qian, Y. Li, Z. H. Wang, *J. Org. Chem.* **2008**, *73*, 7369–7372.
- 25 E. G. Wang, Z. F. Ma, K. Vandewal, P. Henriksson, O. Inganäs, F. L. Zhang, R. A. Andersson, *J. Am. Chem. Soc.* **2011**, *133*, 14244–14247.
- 26 H. J. Chen, Y. L. Guo, G. Yu, Y. Zhao, J. Zhang, D. Gao, H. T. Liu, Y. Q. Liu, *Adv. Mater.* **2012**, *24*, 4618–4622.
- 27 H. J. Chen, Q. Y. Cui, G. Yu, Y. L. Guo, J. Y. Huang, M. L. Zhu, X. J. Guo, Y. Q. Liu, *J. Phys. Chem. C* **2011**, *115*, 23984–23911.
- 28 B. R. Conrad, C. K. Chan, M. A. Loth, S. R. Parkin, X. Zhang, D. M. DeLongchamp, J. E. Anthony, D. J. Gundlach, *Appl. Phys. Lett.* **2010**, *97*, 133306.
- 29 J. G. Liu, Y. Sun, X. Gao, R. B. Xing, L. D. Zheng, S. P. Wu, Y. H. Geng, Y. C. Han, *Langmuir* **2011**, *27*, 4212–4219.
- 30 J. S. Ha, K. H. Kim, D. H. Choi, *J. Am. Chem. Soc.* **2011**, *133*, 10364–10367.